PNAS

Supporting Information for

Strong enhancement of magnetic ordering temperature and structural/valence transitions in $EuPd_3S_4$ under high pressure

Shuyuan Huyan, Dominic H. Ryan, Tyler J. Slade, Barbara Lavina, Greeshma C. Jose, Haozhe Wang, John M. Wilde, Raquel A. Ribeiro, Jiyong Zhao, Weiwei Xie, Wenli Bi, Esen E. Alp, Sergey L. Bud'ko, Paul C. Canfield

Dominic H. Ryan
Email: dominic.ryan@mcgill.ca
Sergey L. Bud'ko
Email: budko@ameslab.gov
Paul C. Canfield
Email: canfield@ameslab.gov

This PDF file includes:

Supporting Information Text

Synchrontron X-ray diffraction

As clearly shown in Fig. S2 (a), the relative intensities of (210) and (211) peaks of the cubic phase ("cubic" is identified as "C") are stable in Zone I, and strongly suppressed in Zone II, accompanied by the emergence of extra peaks at a little higher angle than (210) and (211), which could be (210) and (211) peaks in tetragonal phases ("tetragonal" is identified as "T"). In Zone III, C(210) and C(211) peaks are not detectable anymore, whereas T(210) and T(211) survive with very low relative intensities. The diffraction peaks' positions and relative intensities of (200) and [(210)&(211)] as a function of pressure are plotted in Fig. S2 (b), (c) and (d), (e), respectively. The relative peak intensities are in percents and are obtained by first removing the background and diffraction peaks of copper and rhenium from the spectra and then normalizing the spectra to the diffraction peak with the highest intensity. The peak positions of (200), (210) and (211) in both cubic or tetragonal phases show almost linear behavior as a function of pressure in Zones I and III. Above ~26 GPa, the peak position of (200) shows a small jump to higher angle, and a second jump happens just at ~34 GPa. On the other hand, C(210) and C(211) coexist with T(210) and T(211) peaks in Zone II, and the peaks' positions are almost independent of pressure. The different evolution of peak position in Zone II indicates the possible existence of strain effect between two distinct phases or/and the different compressibility of different phases. As for the peaks' intensities, C(210) and C(211) decrease rapidly from almost 100 % to 0 in zone II, whereas T(210) and T(211) peaks decrease from ~ 25 % to less than 10 % in Zone II and become almost constant. Although there appears to be an increase in intensity in zone III, however, the systematic evolution of (200) peak with pressure is difficult to observed because C(200) peak actually splits into 2 peaks T(200) and T(002) under high pressure and these two peaks are very close to each other, as shown in the inset of Fig. S2 (c). More typical case of peak splitting will be discussed later.

In Fig. S3 (a), we show that a new peak with the peak position around 14.2° (T(113) according to our indexing) emerges at ~20 GPa and systematically shifts to the higher angle with pressure increase. The peak position evolves linearly with the pressure above ~32 GPa and deviates a little bit from a linear relation in the pressure region between ~20 GPa and ~32 GPa, shown in Fig. S3 (b). The intensity of T(113) increases with the pressure rapidly from ~20 GPa to ~32 GPa and it becomes the strongest diffraction peak at higher pressure, as shown in Fig. S3 (c).

Fig. S4 (a) shows that the C(400) peak splits into two peaks i.e. T(400) and T(004) above 27 GPa. A mixed phase is also observed in Zone II, where we can see several small peaks merging together at around the angle of C(400). The accurate information of peak positions and intensities of C(400), T(400) and T(004) could not be obtained in Zone II, whereas in Zone III, clear and well separated T(400) and T(004) peaks are observed. The peak splitting also happens to lower angle diffraction peaks that have small splitting angle such as in C(200). The peak splitting under high pressure suggests that the structure has changed to lower symmetry which is consistent with the suggestion of a cubic to tetragonal structural transition.

Synchrotron Mössbauer spectroscopy

Way to calibrate the absolute value of isomer shifts with EuS as reference. As shown in Fig. S9, at several pressure points, the reference sample EuS, at room temperature and ambient pressure was placed together with $EuPd_3S_4$, which is at 50 K. The collected time-domain spectra were then fitted with CONUSS [1] by fixing the isomer shift of Eu^{2+} site of EuS as -11.496 mm/s, and varying isomer shifts and their weights of all Eu sites of $EuPd_3S_4$ (2 sites below 27 GPa, and 1 site at and above 27 GPa). Since Eu^{2+} peak (as demonstrated in Fig. 4(b)) is more sensitive to pressure. The black circles are the fitted points of isomer shift of Eu^{2+} calibrated by EuS. The black circles can be well fitted with an exponential function shown with the red dashed curve. The detailed fitted parameters are shown in the inset. According to the fitting, we can estimate that the isomer shift of Eu^{2+} is about ~10.75 mm/s at ambient pressure, which is supposed to be the isomer shift of Eu^{2+} and is very close to the reported value (~10.9 mm/s) [2]. The time-domain spectra, collected without reference sample, were fitted by fixing the isomer shift of Eu^{3+} site of $EuPd_3S_4$ as 0 mm/s, and varying isomer shift and the weight of Eu^{2+} sites of $EuPd_3S_4$ (below 27 GPa). The blue circles are the relative isomer shifts of Eu^{2+} fitted with this method. Based on the exponential fitting, we suppose that the absolute isomer shifts of Eu^{2+} at different pressures will drop on the red curve. The isomer shifts of Eu^{3+} at different pressures, then, should be equal to the vertical differences between the red curve and blue circles, as $\Delta\delta$, shown in the figure. The detailed plot of the pressure dependence of absolute isomer-shift values is shown in Fig. 4(c).

Way to estimate the mean valence. The mean valence of the sample at various pressures is usually estimated simply by the area of energy domain absorption peaks, based on the assumption that the area of the absorption peaks is proportional of the number of Eu ions in particular valence. The formula we use is:

$$v = \frac{2A_{Eu^{2}} + 3A_{Eu^{3}}}{A_{Eu^{2}} + A_{Eu^{3}}} \quad (1)$$

where v is the mean valence, A is the area.

It is worth noting that the valence fluctuation between the $4f^7$ and $4f^6$ configurations typically occurs on the order of 10^{-11} s [3]. However, Mössbauer spectroscopy operates on a characteristic time scale of approximately 10^{-8} s, which is three orders of magnitude longer than the valence fluctuation time. As a result, Mössbauer spectroscopy may only yield an average isomer shift from the intermediate valence state instead of distinct isomer shifts for Eu^{2+} and Eu^{3+} when the isomer shift of Eu^{2+} begins to shift towards higher energies, indicating an oxidation state approaching 3+. Given that there is already an approximate 50:50 Eu^{2+}:Eu^{3+} at ambient pressure, which is the $EuPd_3S_4$ case, we may observe both separated Eu3+ isomer shift and an average Eu isomer shift under pressure (represented by the Eu^{2+} peak in Fig. 4 and Fig. S7). And using the empirical formula [4], the average isomer shift δ for very short fluctuation times could be expressed by:

$$\delta = p_{Eu^{2+}}\delta_{Eu^{2+}} + p_{Eu^{3+}}\delta_{Eu^{3+}} \quad (2)$$

Where $p_{Eu^{2+}}$ and $p_{Eu^{3+}}$ are the relative populations of the 2+ and 3+ states. $\delta_{Eu^{2+}}\ and\ \delta_{Eu^{3+}}$ are the absolute isomer shift of 2+ and 3+ state. Based on the consistent evolution of isomer shift as a function of the pressure in Fig. 4, it is convenient to fix $\delta_{Eu^{3+}}$ at zero and use the linear fit to estimate the $\delta_{Eu^{2+}}\ and\ \delta_{Eu^{3+}}$. Then the average of valence $v\_$ is given by:

$$v\_ = 3 - \frac{\delta}{\delta_{Eu^{2+}}} \quad (3)$$

Then we can improve the formula (1) as:

$$v = \frac{v\_ \times A_{Eu^{2}} + 3 \times A_{Eu^{3}}}{A_{Eu^{2}} + A_{Eu^{3}}} \quad (4)$$

Fig. 6 (d) shows the mean valence as a function of the pressure after fixing. The estimation is made under the assumption that the pressure effect is small.

SI References

1. W. Sturhahn, CONUSS and PHOENIX: Evaluation of nuclear resonant scattering data. *Hyperfine Interact*. 125, 149-172 (2000).
2. D. H. Ryan, S. L. Bud'ko, B. Kuthanazhi, and P. C. Canfield, Valence and magnetism in $EuPd_3S_4$ and $(Y,La)_xEu_{1-x}Pd_3S_4$, *Phys. Rev. B* 107, 014402 (2023).
3. G. Wortmann, U. Ponkratz, Bi. Bielemeier, and K. Rupprecht, Phonon density-of-states in bcc and hcp Eu metal under high pressure measured by ^{151}Eu nuclear inelastic scattering of synchrotron radiation, *High. Press. Res*. 28, 545–551 (2008).
4. E. R. Bauminger, D. Froindlich, I. Nowik, S. Ofer, I. Felner, and I. Mayer, Charge fluctuations in Europium in metallic $EuCu_2Si_2$, *Phys. Rev. Lett*. 30, 21 (1973).

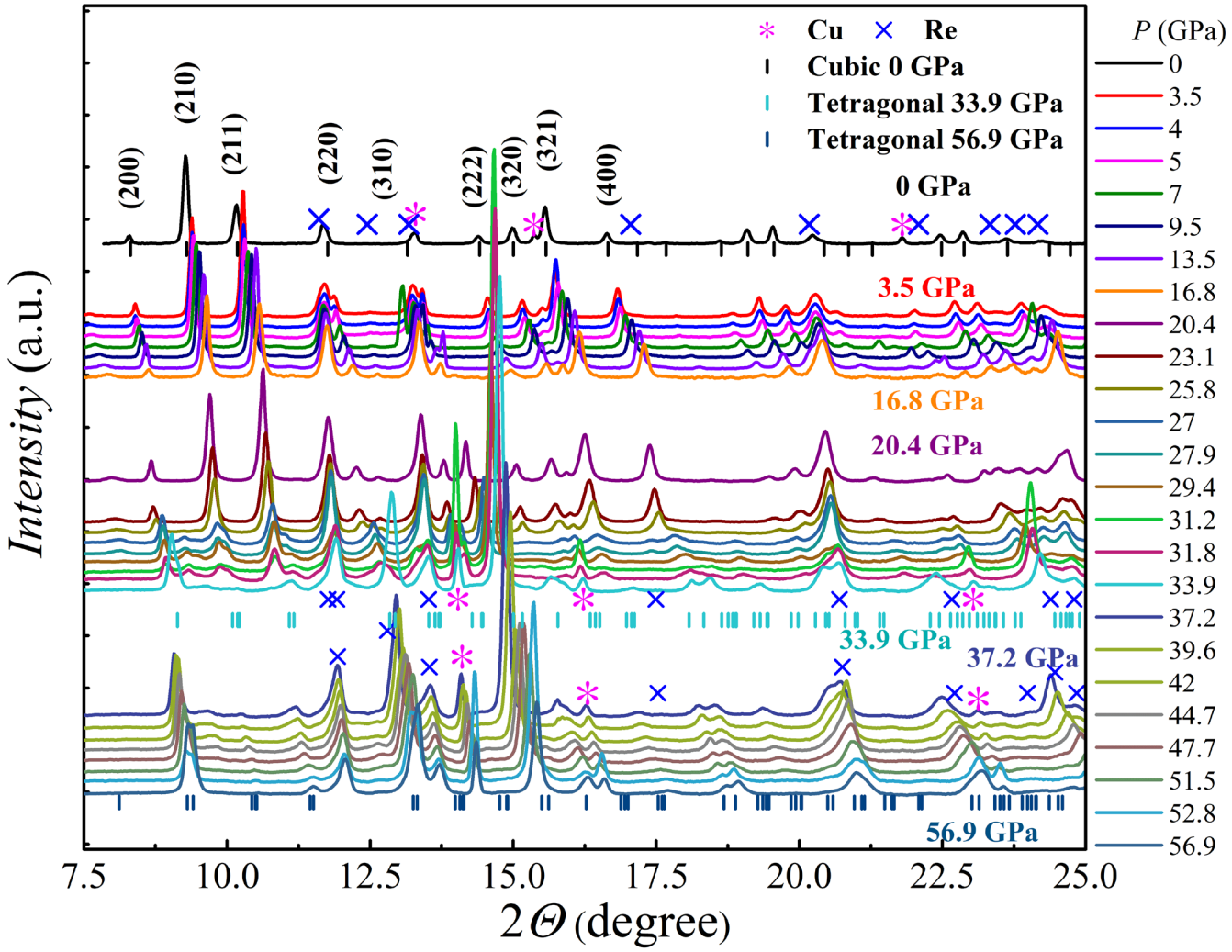

Fig. S1. Pressure induced the structural phase transition. The PXRD patterns of $EuPd_3S_4$ at various pressures from 0 GPa to 56.9 GPa. The synchrotron x-ray wavelength λ is 0.4833 Å. The data are collected at room temperature. The pink stars and blue crosses represent peaks in the PXRD spectra of copper and rhenium, respectively.

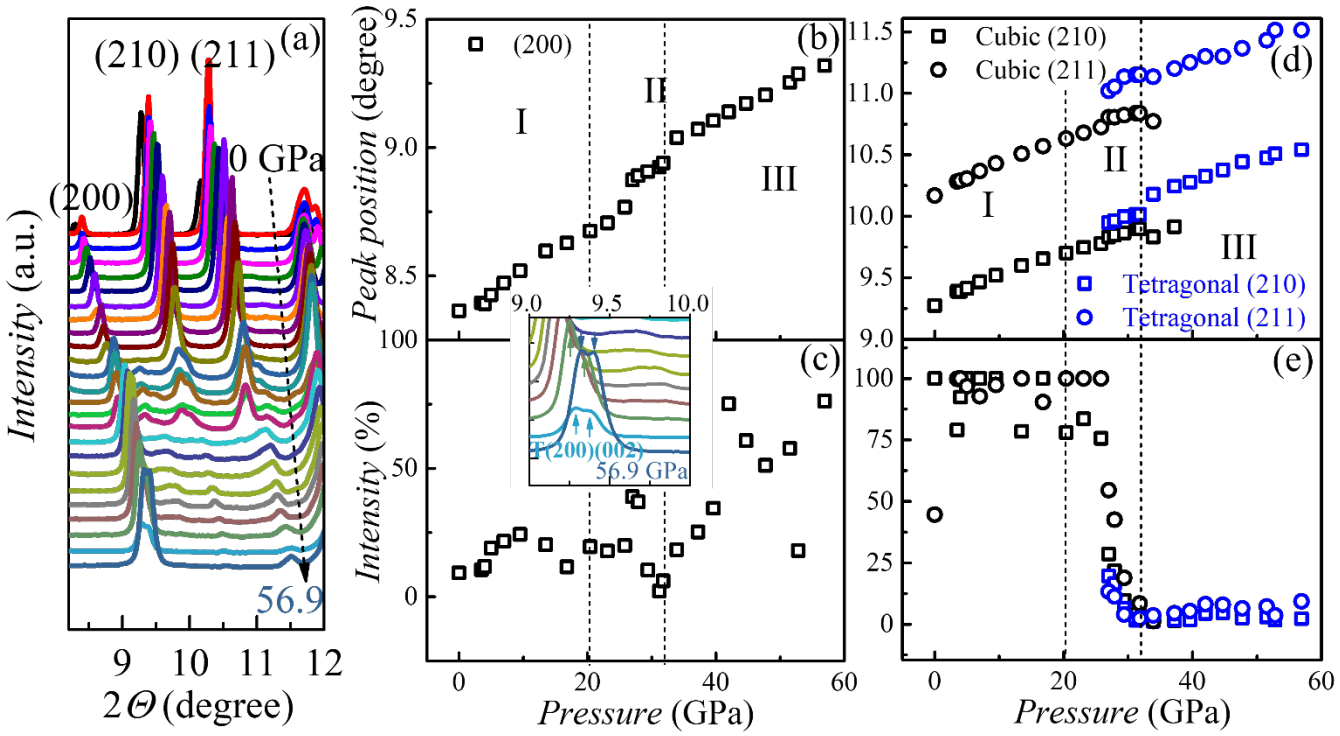

Fig. S2. Demonstration of typical cases for structural phase transition under high pressure in selected 2θ ranges. (a) Showing the evolution of (200), (210) and (211) peaks with the pressure. (a) uses the same legend as Fig. S1. Pressure increases from top (0 GPa) to bottom (56.9 GPa). (b) and (d) Diffraction peaks positions of (200), (210) and (211) as a function of pressure. (c) and (e) Relative intensity of (200), (210) and (211) peaks as a function of pressure. The inset in (c) is a zoomed view of the pattern showing the peak splitting from cubic (200) to tetragonal (200) and (002). The pressure region between the two dashed lines corresponds to the two-phase region where both cubic and tetragonal phases are present.

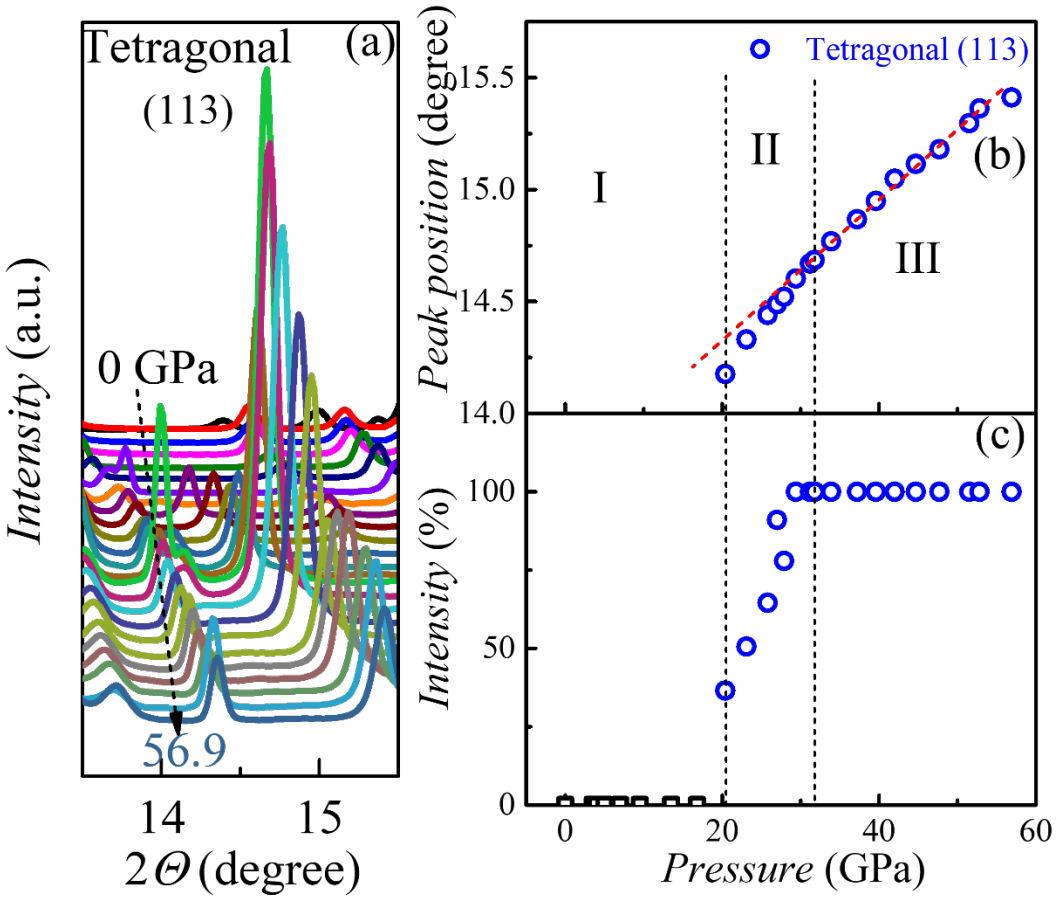

Fig. S3. Demonstration of typical cases for structural phase transition under high pressure in selected 2θ ranges: new peak emergence. (a) The new peak (possible tetragonal (113)) appears under high pressure. (a) uses same legend as Fig. S1. Pressure increases from top (0 GPa) to bottom (56.9 GPa). (b) Diffraction peak position of possible (113) in tetragonal phase as a function of pressure. (c) Relative intensity of (113) peak as a function of pressure. The pressure region in between two dashed lines might be in a two-phase region of the cubic phase and tetragonal phase. The red dashed straight line is a guide to the eye.

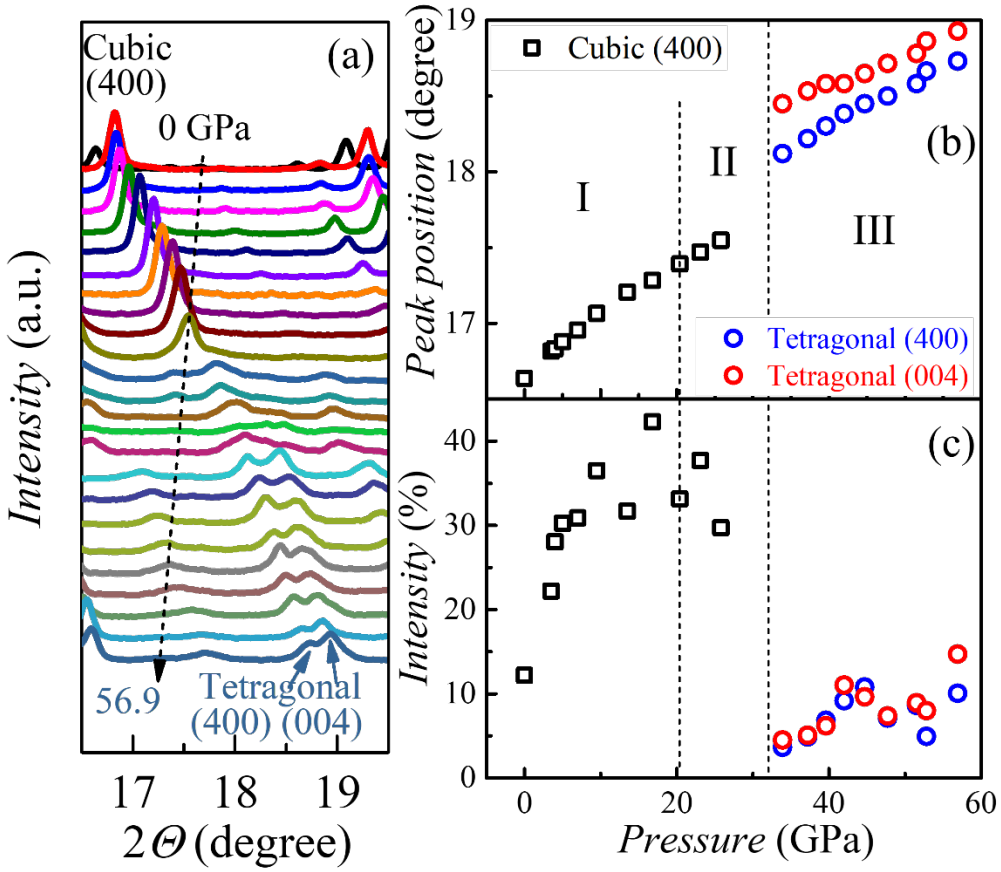

Fig. S4. Demonstration of typical cases for structural phase transition under high pressure in selected 2θ ranges: peak splitting. (a) The cubic (400) Bragg peak splits into tetragonal (400) and (004) peaks under high pressure. (a) uses same legend as Fig. S1. Pressure increases from top (0 GPa) to bottom (56.9 GPa). (b) Diffraction peak positions of the cubic (400) peak and the tetragonal (400) and (004) peaks as a function of pressure. (c) Relative intensities of the cubic (400) and tetragonal (004) peaks as function of pressure. The pressure region in between two dashed lines contains a mixture of cubic and tetragonal phases.

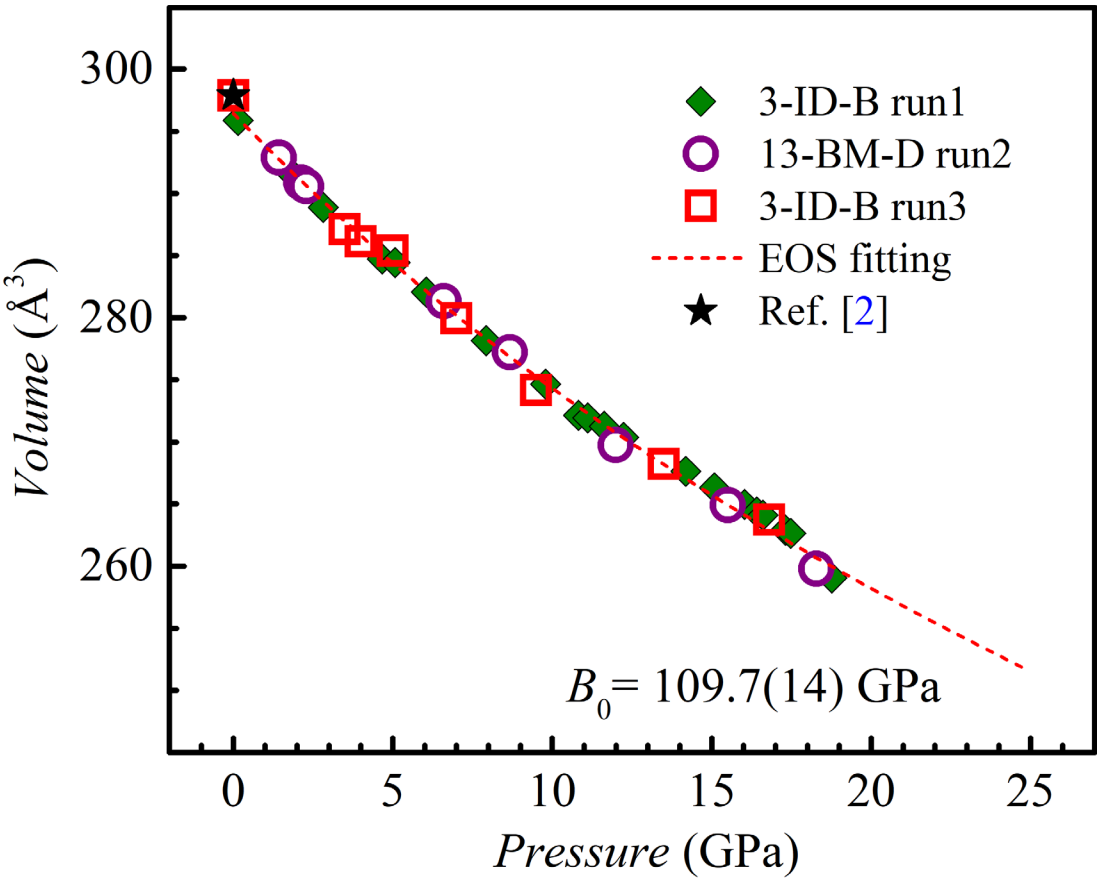

Fig. S5. The consistency in volume evolution with pressure in zone I. The unit cell volume as a function of pressure, based on several independent runs of PXRD measurements (run1 to run3). All PXRD data are put together and could be fitted well with a second-order BM EOS (shown by red dashed curve), with zero-pressure volume V_0= 296.54 Å^3, which is close to the previous report value (~297.9 Å^3) [2], and zero-pressure bulk modulus B_0=109.7(14) GPa. This figure clearly shows the agreement between different runs.

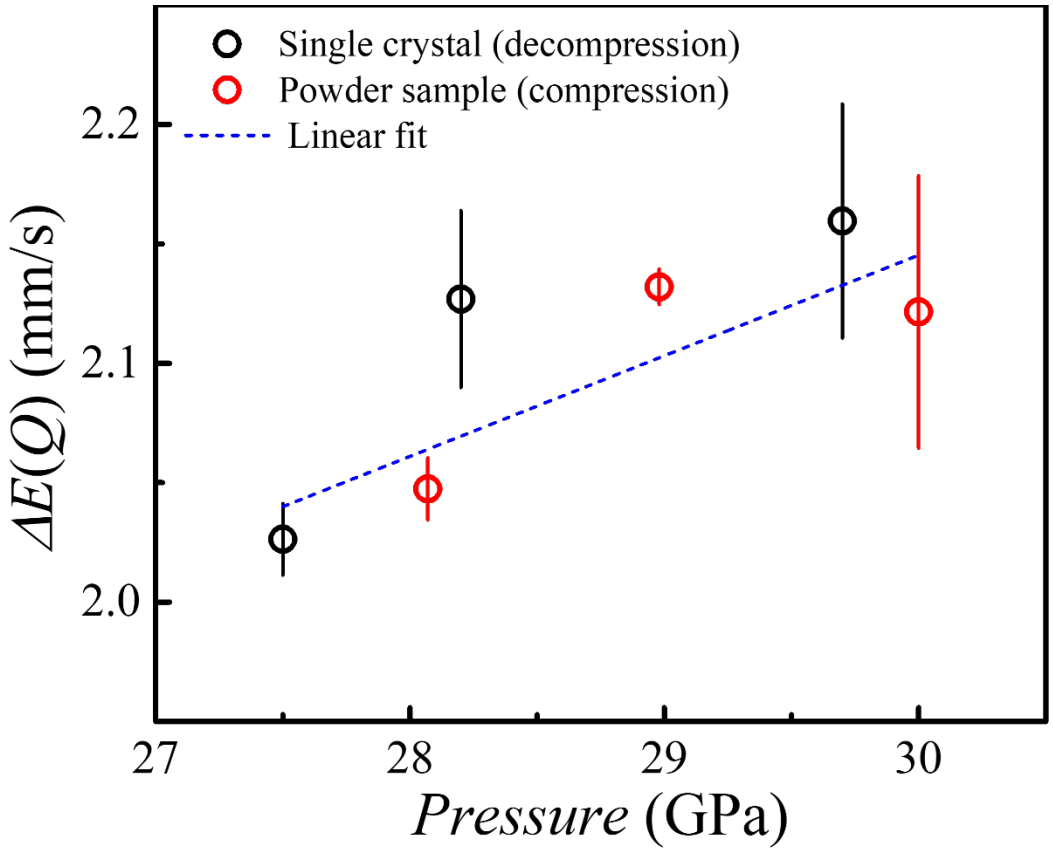

Fig. S6. Pressure dependence of quadrupole interaction, *ΔE*(*Q*). When the valence transition occurs, a distinct change was observed in the time-domain Mössbauer spectra, indicating the disappearance of Eu^{2+}. The spectra can be accurately fitted by introducing a quadrupole splitting term at the Eu^{3+} site, attributed to the presence of an electric field gradient in the lower symmetry, tetragonal unit cell. As such then, this observation aligns effectively with the structural transition from cubic to tetragonal. Meanwhile, it is noted that the quadrupole interaction tends to have small amount of increase with the pressure at the range between ~28 and ~30 GPa.

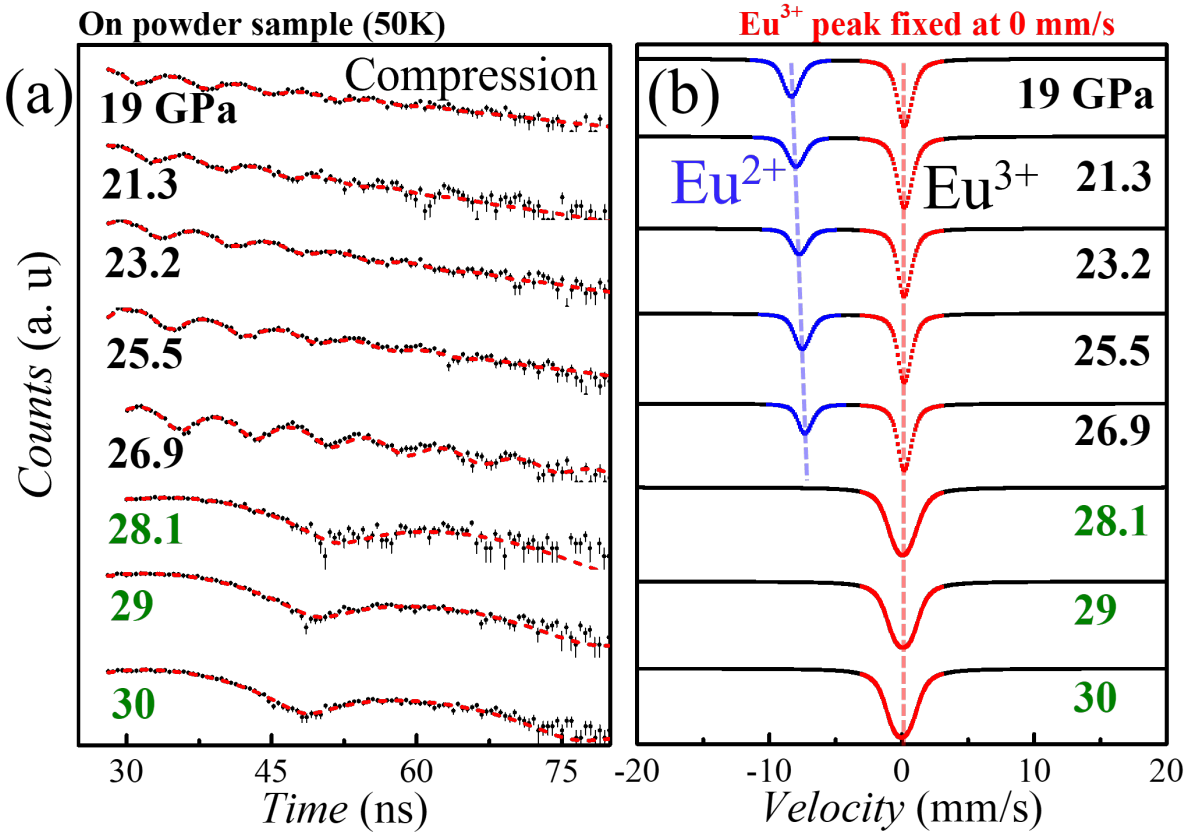

Fig. S7. Pressure induced Eu valence transition from the isomer shift. (a) The Synchrotron Mössbauer spectroscopy spectra (SMS) in time domain of ^{151}Eu from $EuPd_3S_4$ at 50 K under different pressures on sintered powder sample. The red curves show the fit of the SMS spectra. (b) Simulated energy-domain Mössbauer spectra based on the fitting results from each corresponding SMS spectrum. (a) and (b) share the same legend.

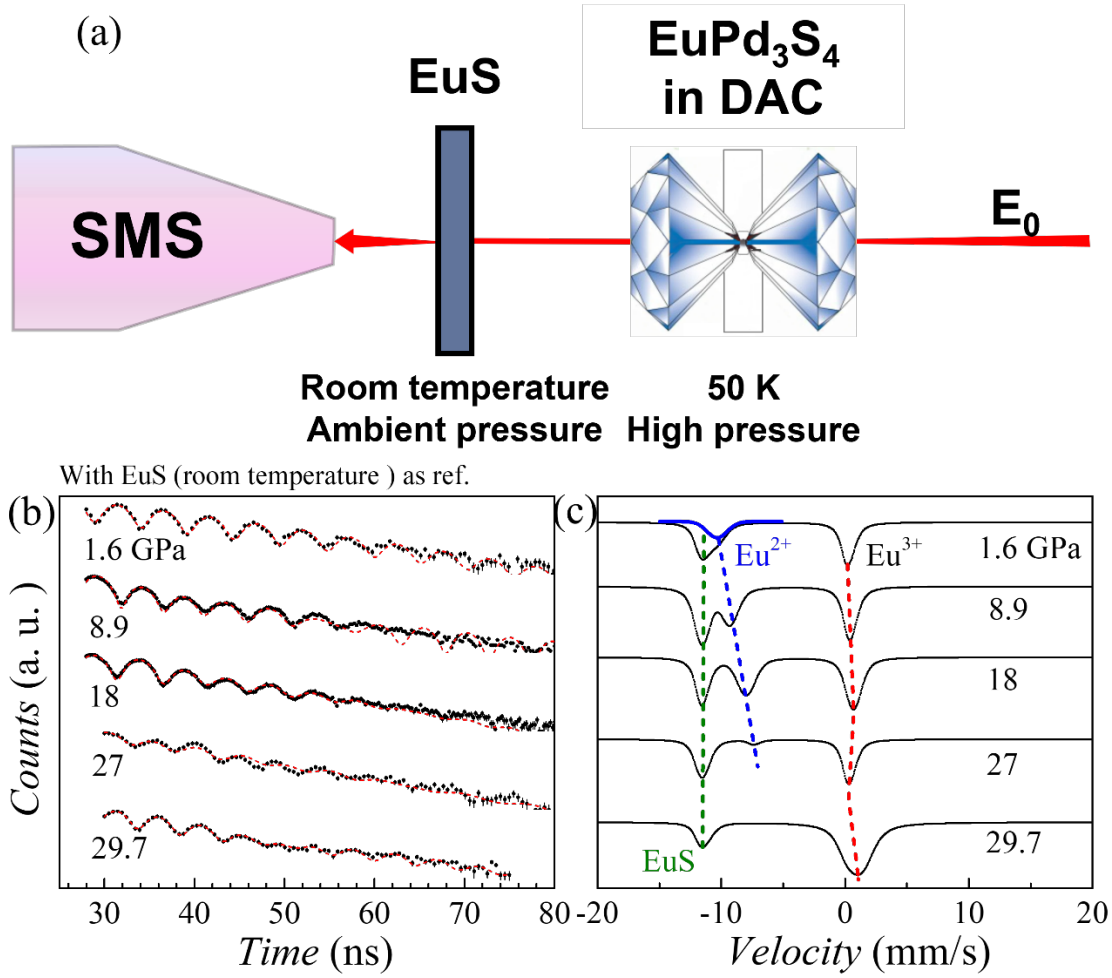

Fig. S8. Calibration of the absolute value of isomer shifts with EuS as reference. (a) Schematic drawing of the SMS measurement setup with reference sample EuS. (b) The SMS spectra in the time domain of ^{151}Eu from $EuPd_3S_4$ at 50 K at various pressures, obtained from experimental measurements conducted on a single crystal sample. To determine the absolute value of the isomer shift and its variation with applied pressure, a reference sample of EuS is employed at room temperature. The red dashed curves represent the fittings of the SMS spectra. (c) Energy-domain spectra simulations are performed based on the fitted results obtained from each corresponding time-domain SMS spectrum. The green dashed line indicates the isomer shift of Eu^{2+} of the reference sample EuS, which remains fixed at -11.496 mm/s. The blue and black dashed lines serve as visual guides illustrating the evolution of the Eu^{2+} and Eu^{3+} peaks of $EuPd_3S_4$, respectively, as pressure increases. This depiction agrees with the results depicted in Fig. 4(b). The blue Gaussian peak observed just above 1.6 GPa corresponds to the fitted peak of the Eu^{2+} peak in $EuPd_3S_4$. Both (a) and (b) share the same legend.

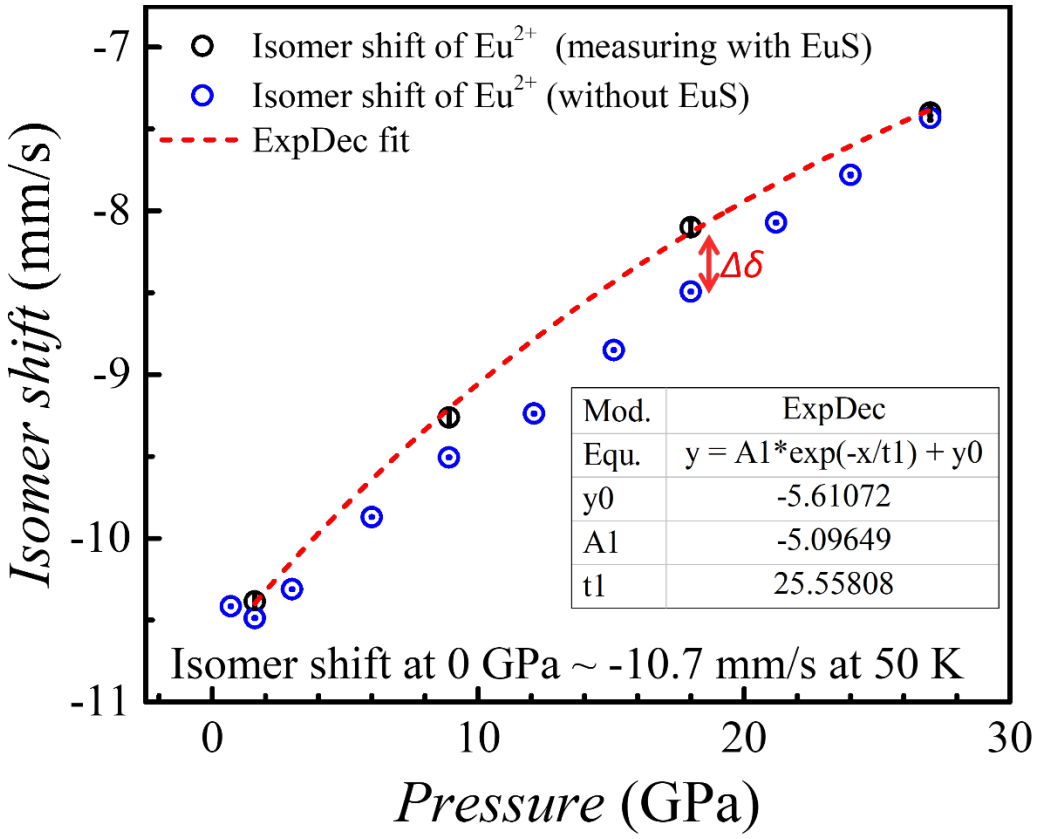

Fig. S9. Calibration of the absolute value of isomer shifts with EuS as reference.

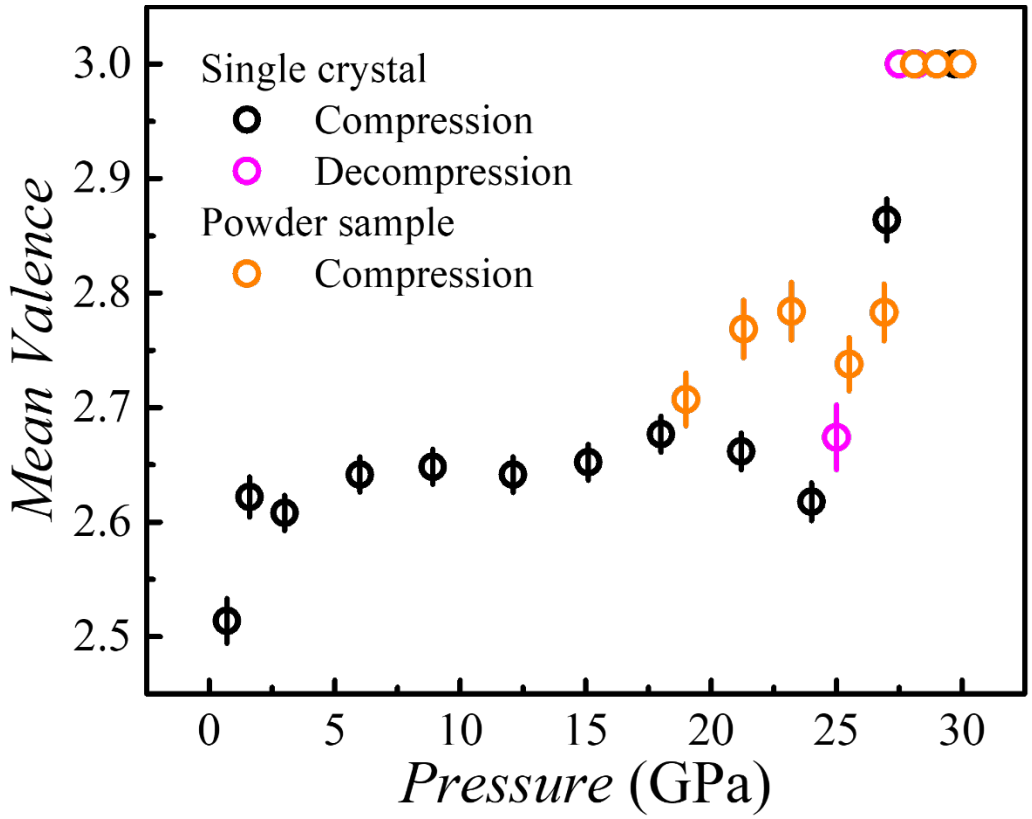

Fig. S10. Mean valence estimated by the areas of the absorption peaks assuming that above the critical pressure of valence transition, the absorption peak with negative isomer shift is assumed to be an average peak with partial Eu^{2+} and Eu^{3+} due to the valence fluctuation.